

# LOW POWER RF TEST OF A QUADRUPOLE-FREE X-BAND MODE LAUNCHER FOR HIGH BRIGHTNESS APPLICATIONS

G. Torrissi\*, G. Sorbello<sup>1</sup>, L. Celona, O. Leonardi, G. Mauro and S. Gammino  
INFN-LNS, Catania, Italy

<sup>1</sup>also at University of Catania, Catania, Italy

G. Castorina, Bruno Spataro, INFN-LNF, Frascati, Italy

L. Faillace, INFN-Milan, Milan, Italy

V. Dolgashev, SLAC, Menlo Park, USA

## Abstract

In this work we present the low power RF characterization of a novel  $TM_{01}$  X-band mode launcher for the new generation of high brightness RF photo-injectors. The proposed mode launcher exploits a fourfold symmetry which minimizes both the dipole and the quadrupole fields in order to mitigate the emittance growth in the early stages of the acceleration process. Two identical aluminum mode launchers have been assembled and measured in back-to-back configurations for three different central waveguide lengths. From the back-to-back results we infer the performance of each mode launcher. The low power RF test, performed at the Istituto Nazionale di Fisica Nucleare Laboratori Nazionali del Sud (INFN-LNS), validate both the numerical simulations and the quality of fabrication. An oxygen-free high-conductivity copper version of the device is being manufactured for high power and ultra high vacuum tests that are planned to be conducted at SLAC.

## INTRODUCTION AND MOTIVATION

The R&D of high gradient radiofrequency (RF) devices is aimed to develop innovative accelerating structures and achieve higher accelerating gradient in order to increase brilliance of accelerated bunches. Recent research has shown that accelerating gradients up to 250 MV/m are feasible using cryogenically cooled copper accelerating structures [1,2]. A high brilliance requires high field quality in the RF photoguns and in its power coupler. Moreover, the higher is the electric field on the cathode surface of the gun the lower the beam emittance [3–6]. This lower emittance could be degraded by the multipole components of the gun electromagnetic fields. In this work we present a novel X-band power coupler which consists of a  $TM_{01}$  Mode Launcher (ML) (from the rectangular  $TE_{10}$  mode to the circular  $TM_{01}$  mode [7]), with a fourfold symmetry which minimized both the dipole and the quadrupole RF components [8]. The device was developed in the frame of the collaboration with INFN-LNF and SLAC (USA); low power RF measurements, performed in the framework of the DiElectric and METallic Radiofrequency Accelerator (DEMETRA) activities and conducted at INFN-LNS, are discussed in the paper. In particular we will show the low-power-microwave tests of two identical MLs joined back-to-back. This configuration

allows a direct measurement of S-parameters using a two-port vector network analyzer (VNA), Agilent N5230A 10 MHz-50 GHz, Agilent Technologies.

## MODE LAUNCHER RF DESIGN

The proposed X-band ML design is based on four symmetric sidewall coupling apertures that reduce the converter length and allow on-axis power coupling of the azimuthally symmetric  $TM_{01}$  mode. The symmetry of the configuration removes all non-fourfold symmetric modes i.e. dipolar modes (as the standard mode launcher does) and quadrupole components [9].

In our case, in order to couple a TM mode, the branching network lays in the H-plane: the adopted original and compact layout, shown in Fig. 1 and simulated with the Ansys HFSS code [10], keeps the maximum surface electric and magnetic fields sufficiently low to guarantee multi-MW delivery (200 MW) to a device of this structure.

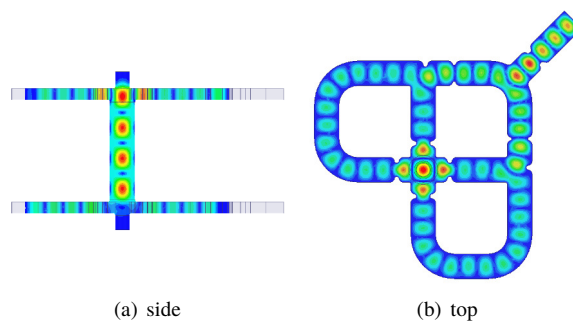


Figure 1: Side and Top view of the longitudinal (beam-axis) Electric field component  $E_y$  of simulated back-to-back MLs.

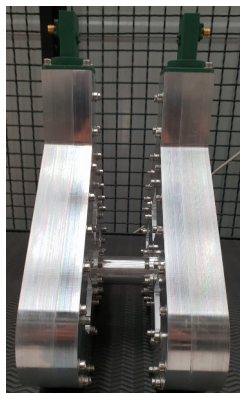
Details on the  $TM_{01}$  mode launcher feeding layout, the delay line to match the phase at the sidewall coupling apertures, and matching bumps can be found in [8]. The H-plane branching network has been optimized with a reduced model [11] which takes advantage of symmetry [11–13] to reduce the computational domain.

## FABRICATION AND LOW-POWER-MICROWAVE TESTS

Figure 2(a) shows the final assembled identical MLs in back-to-back configuration. Each ML is composed of two separate metal aluminum halves: a milled plate where the

\* giuseppe.torrissi@lns.infn.it

waveguide branching is machined (see Fig. 2(b)) and a plane cover. The milling of aluminum blocks has been operated [14] using a tolerance of  $10\ \mu\text{m}$  and a surface roughness of  $100\ \text{nm}$ . Being the “low-power-microwave test” aluminum structure based on two pieces, it requires a large number of screws to ensure good rf contact. During the device assembling, care should be taken to ensure the flange screws are symmetrically tightened in order to obtain a good electrical contact and alignment between the two pieces. When the two halves are joined together, they form the complete ML. Two identical aluminum prototypes (Fig. 2(c)) have been fabricated and measured in three back-to-back configurations for three different circular waveguide connection lengths (3, 6 and 12 cm) through a well-calibrated (Keysight X11644A Mechanical WR90 Waveguide Calibration Kit, 8.2 to 12.4 GHz, WR-90) VNA.



(a) Manufactured Mode Launchers connected back-to-back by a circular waveguide of length 6 cm



(b) Slotted plane of the Mode Launcher.

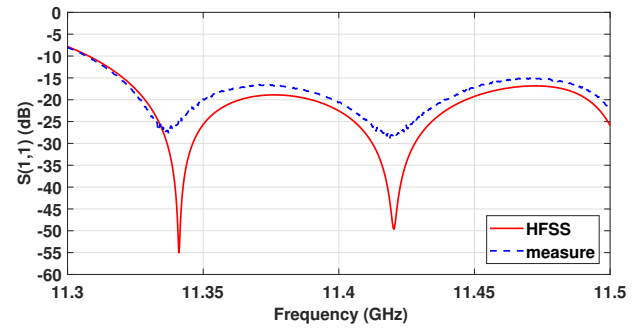


(c) Two identical fabricated MLs for back-to-back measurement.

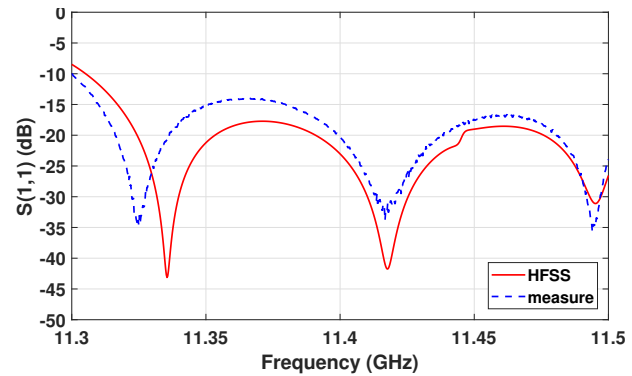
Figure 2: Photos of the manufactured aluminum Mode Launchers for low-power-microwave tests.

Figures 3 and 4 show the comparison between the simulated and experimental scattering parameters ( $|S_{11}|$  and  $|S_{12}|$  respectively) of the X-band  $\text{TM}_{01}$  MLs back-to-back connected. The sub-figures (a), (b), (c) show this comparison for the three different circular waveguide central sections of length 3 cm, 6 cm and 12 cm respectively.

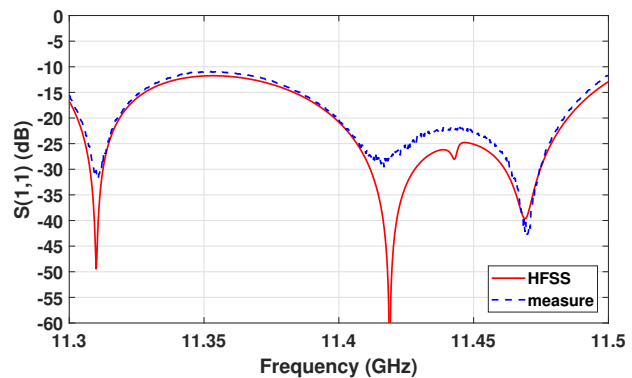
The device is well matched,  $|S_{11}|$  below  $-10\ \text{dB}$ , in the frequency range 11.3-11.5 GHz; at the operating frequency



(a)  $l = 32\ \text{mm}$



(b)  $l = 62\ \text{mm}$



(c)  $l = 122\ \text{mm}$

Figure 3: Comparison of measured and simulated reflection coefficient  $|S_{11}|$  for the full devices in back-to-back configuration. At the working frequency  $|S_{11}|$  is about  $-30\ \text{dB}$ .

11.42 GHz,  $|S_{11}|$  is about  $-25\ \text{dB}$  for all the three connected sections.

Back-to-back measurement shows that the averaged loss of the mode launcher is about 0.2 dB higher than that of the simulation. This is likely due to the losses resulting from imperfect electrical contact in this low-power-microwave test prototypes. We do not expect this discrepancy in a brazed device. In the measurement, we can also observe secondary peaks in the  $S$  parameters. They are caused by the resonant cavities between the two identical launchers: it can be seen that by changing the distance between the ML, the resonant frequencies of the peaks shift, as observed in [15, 16].

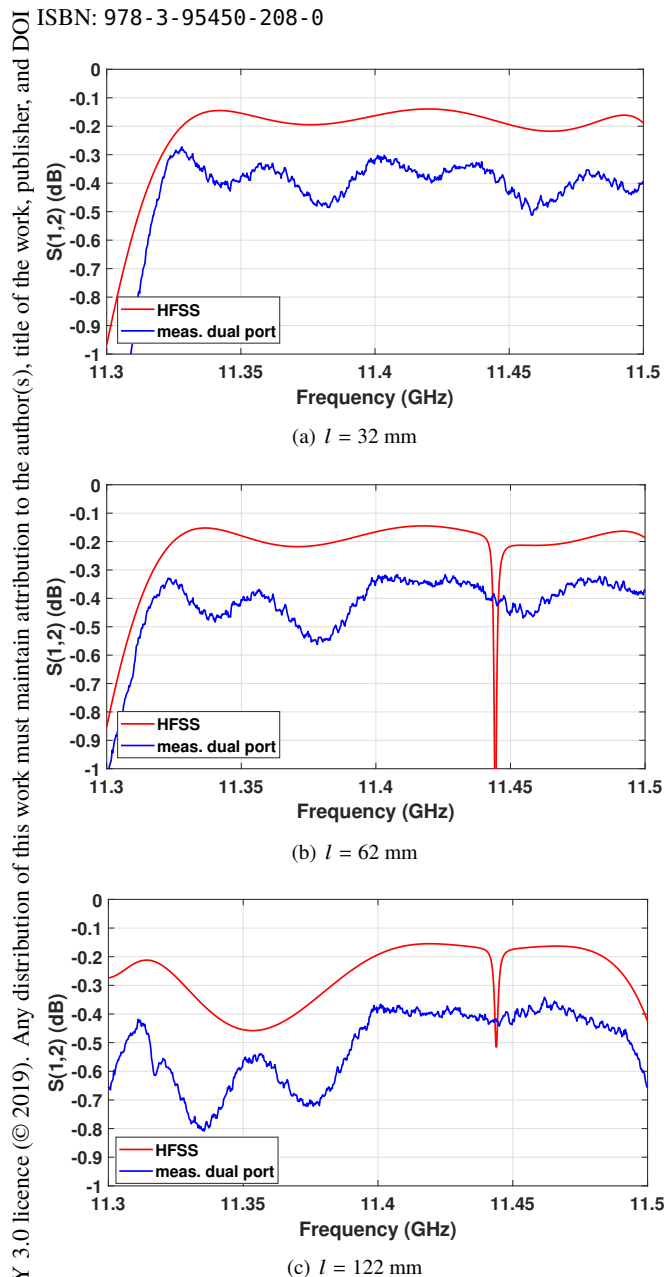
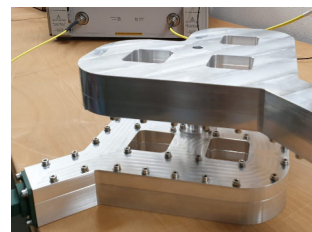


Figure 4: Comparison of measured and simulated Transmission coefficient  $|S_{12}|$  for the full devices in back-to-back configuration. At the working frequency  $|S_{12}|$  is  $-0.4$  dB.

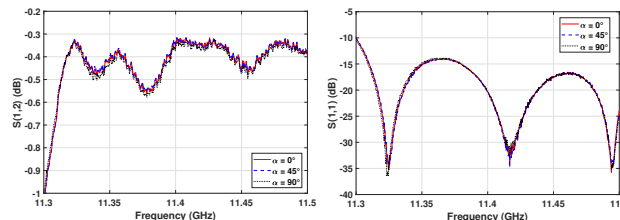
In order to further explore the field symmetry and to examine the existence of competing quadrupolar modes, three measurements have been made by rotating the second ML of the angle  $\theta=0^\circ, 45^\circ$  ad  $90^\circ$ . The setup for the position  $\theta=90^\circ$  is shown in Fig. 5(a). Fig. 5(b) clearly shows that the measured results of  $S$ -parameters are independent of the angle for the operating bandwidth. Back-to-back low-power-microwave tests show good performance and agrees well with simulations.

### CONCLUSION

A novel RF power coupler for RF photoinjector designed for high brightness applications has been presented. The de-



(a) Photo of the two mode-launchers jointed back to back and rotated at an angle  $\theta=90^\circ$ .



(b)  $S$ -parameter measurement for three angles

Figure 5: Measurements of modal symmetry/purity.

sign could be used with both room temperature photoinjector, and as a part of a cryostat assembly for normal-conducting cryogenic structures. As an example of the mode-launcher usage you can refer to [17]. The proposed mode launcher is a X-band  $TM_{01}$  waveguide mode launcher which minimizes dipole and quadrupole field components. The low-power-microwave mode launcher has been fabricated and tested. This launcher features good back-to-back performances. We plan to test a brazed version of this mode launcher at high power at SLAC.

### Acknowledgments

This work is supported by INFN V Nat. committee under the DEMETRA grant. We wish to acknowledge the support of S. Passarello for the mechanical drawing and design of the manufactured items.

## REFERENCES

- [1] A. D. Cahill, J. B. Rosenzweig, V. A. Dolgashev, S. G. Tantawi, and S. Weathersby, "High gradient experiments with x-band cryogenic copper accelerating cavities," *Phys. Rev. Accel. Beams*, vol. 21, p. 102002, Oct 2018.
- [2] D. Alesini *et al.*, "Design of high gradient, high repetition rate damped c-band rf structures," *Phys. Rev. Accel. Beams*, vol. 20, p. 032004, Mar 2017.
- [3] A. Cianchi *et al.*, "High brightness electron beam emittance evolution measurements in an rf photoinjector," *Phys. Rev. ST Accel. Beams*, vol. 11, p. 032801, Mar 2008.
- [4] A. Cianchi *et al.*, "Six-dimensional measurements of trains of high brightness electron bunches," *Physical Review Special Topics - Accelerators and Beams*, vol. 18, 08 2015.
- [5] D. Filippetto *et al.*, "Phase space analysis of velocity bunched beams," *Phys. Rev. ST Accel. Beams*, vol. 14, p. 092804, Sep 2011.
- [6] J. Rosenzweig *et al.*, "Ultra-high brightness electron beams from very-high field cryogenic radio-frequency photocathode sources," *Nuclear Instruments and Methods in Physics Research Section A: Accelerators, Spectrometers, Detectors and Associated Equipment*, 01 2018.
- [7] C. Nantista, S. Tantawi, and V. Dolgashev, "Low-field accelerator structure couplers and design techniques," *Phys. Rev. ST Accel. Beams*, vol. 7, p. 072001, Jul 2004.
- [8] G. Castorina *et al.*, "TM<sub>01</sub> mode launcher with quadrupole field components cancellation for high brightness applications," *J. Phys.: Conf. Ser.*, p. 1067 082025, 2018.
- [9] T.-H. Chang, C.-H. Li, C.-N. Wu, and C.-F. Yu, "Generating pure circular TE<sub>mn</sub> modes using Y-type power dividers," *IEEE Transactions on Microwave Theory and Techniques*, vol. 58, no. 6, pp. 1543–1550, 2010.
- [10] "ANSYS HFSS, 3D full-wave electromagnetic field simulation by Ansoft,"
- [11] G. Castorina, G. Torrissi, G. Sorbello, L. Celona, and A. Mostacci, "Conductor losses calculation in two-dimensional simulations of h-plane rectangular waveguides," *J. of Electromagnet. Wave*, pp. 1–10, 2019.
- [12] A. F. Oskooi, D. Roundy, M. Ibanescu, P. Bermel, J. D. Joannopoulos, and S. G. Johnson, "MEEP: a flexible free-software package for electromagnetic simulations by the FDTD method," *Computer Physics Communications*, vol. 181, no. 3, pp. 687–702, 2010.
- [13] M. Aloisio and G. Sorbello, "One-third-of-pitch reduction technique for the analysis of ternary azimuthally periodic helical slow-wave structures," *IEEE Trans. Electron Devices*, vol. 53, no. 6, pp. 1467–1473, 2006.
- [14] "Co.me.b srl,"
- [15] G. Liu *et al.*, "A millimeter wave high-order te<sub>13</sub> mode converter," *IEEE Trans. Electron Devices*, vol. 63, pp. 1–5, 05 2016.
- [16] C.-F. Yu and T.-H. Chang, "High-performance circular TE<sub>01</sub>-mode converter," *IEEE Trans. Microw. Theory Tech*, vol. 53, pp. 3794 – 3798, 01 2006.
- [17] W. Graves, V. Bharadwaj, P. Borchard, V. Dolgashev, A. Goodrich, M. Holl, E. Nanni, and N. O'Brien, "Design of an X-Band Photoinjector Operating at 1 kHz," in *Proceedings, 8th International Particle Accelerator Conference (IPAC 2017): Copenhagen, Denmark, May 14-19, 2017*, p. TU-PAB139, 2017.